

Article

Forecasting Urban Land Use Change Based on Cellular Automata and the PLUS Model

Linfeng Xu ¹, Xuan Liu ², De Tong ^{3,*}, Zhixin Liu ¹, Lirong Yin ⁴ and Wenfeng Zheng ⁵

¹ School of Life Science, Shaoxing University, Shaoxing 312000, China; linfeng.xu@usx.edu.cn (L.X.); liuzhixin@usx.edu.cn (Z.L.)

² School of Public Affairs and Administration, University of Electronic Science and Technology of China, Chengdu 610054, China; liuxuan@uestc.edu.cn

³ Laboratory for Urban Future, Peking University Shenzhen Graduate School, Shenzhen 518055, China

⁴ Department of Geography and Anthropology, Louisiana State University, Baton Rouge, LA 70803, USA; lyin5@lsu.edu

⁵ School of Automation, University of Electronic Science and Technology of China, Chengdu 610054, China; winfirms@uestc.edu.cn

* Correspondence: tongde@pkusz.edu.cn

Abstract: Nowadays, cities meet numerous sustainable development challenges in facing growing urban populations and expanding urban areas. The monitoring and simulation of land use and land-cover change have become essential tools for understanding and managing urbanization. This paper interprets and predicts the expansion of seven different land use types in the study area, using the PLUS model, which combines the Land use Expansion Analysis Strategy (LEAS) and the CA model, based on the multi-class random patch seed (CARS) model. By choosing a variety of driving factors, the PLUS model simulates urban expansion in the metropolitan area of Hangzhou. The accuracy of the simulation, manifested as the kappa coefficient of urban land, increased to more than 84%, and the kappa coefficient of other land use types was more than 90%. To a certain extent, the PLUS model used in this study solves the CA model's deficiencies in conversion rule mining strategy and landscape dynamic change simulation strategy. The results show that various types of land use changes obtained using this method have a high degree of accuracy and can be used to simulate urban expansion, especially over short periods.

Keywords: urban expansion; LEAS; CARS; land use interpretation; China



Citation: Xu, L.; Liu, X.; Tong, D.; Liu, Z.; Yin, L.; Zheng, W. Forecasting Urban Land Use Change Based on Cellular Automata and the PLUS Model. *Land* **2022**, *11*, 652. <https://doi.org/10.3390/land11050652>

Academic Editors: Yanliu Lin and Yan Guo

Received: 5 April 2022

Accepted: 25 April 2022

Published: 28 April 2022

Publisher's Note: MDPI stays neutral with regard to jurisdictional claims in published maps and institutional affiliations.



Copyright: © 2022 by the authors. Licensee MDPI, Basel, Switzerland. This article is an open access article distributed under the terms and conditions of the Creative Commons Attribution (CC BY) license (<https://creativecommons.org/licenses/by/4.0/>).

1. Introduction

Since 2014, more than half of the world's population now live in urban areas, and this proportion is expected to increase to 66 percent by 2050 (UN, 2018) [1]. Cities face numerous challenges in meeting the needs of their growing urban populations, and managing urban areas has become one of the most critical development challenges worldwide [2]. Monitoring and simulating land use and land cover (LULC) are important for understanding the trend of urbanization within an area [3], as they can indicate anthropogenic impacts, identify land use problems such as degradation and deforestation, and act as basic supporting information for land use plans aiming towards the sustainable development of a city [4].

Presently, three key areas advocate new research internationally on LULC: (1) The temporal and spatial changes in land use. The application of remote sensing and GIS technology allows scholars to catch up with land use changes throughout the world [5]. Evidence all over the world has illustrated the uneven distribution of land use changes in different areas, from European countries [6] to western Kenya [7], and eastern China [8]. (2) The environmental impact of land use. Scholars began to link land use changes with air pollution [9–11], temperature change [12,13], water-logging disasters [14], and so on. (3) The driving force of land use change. Current driving factors of global LUCC mainly focus on

population, culture, economic and political structures, technology, and distribution [15]. For the lattermost, weighing the importance of various factors to cover change and obtaining the correlation between factors for land use prediction have caught scholars' attention. A new method is urgently needed.

The establishment of correlation analysis between land use types, driving factors, and empirical diagnosis models to obtain and predict cover changes are proposed, with the support of computer technologies. This problem is partially solved with cellular automata (CA) [16]. CA is a dynamic model in which space-time and its state are both discrete. It describes multi-agent interactions and has been extensively applied to model spatiotemporal land use dynamics under the influences of natural and socioeconomic factors, including their interactions at different scales [17,18]. However, currently, CA is affected by specific spatial patterns, due to the definition of rules, and cannot be applied universally [19]. Additionally, most existing CA models pay too much attention toward improving simulation technology and correcting conversion rules. Furthermore, little attention has been paid toward the need for a more conceptual understanding of the underlying causes of LULC [20].

Therefore, for decision-makers, the existing CA models often: (1) play a limited role in exploring the causes of land use changes [21], and (2) experience difficulties when dynamically simulating patch-level changes of multiple land use types in time and space [22]. This is especially true for natural land types, such as woodland and grassland. The existing CA models have certain deficiencies in the conversion rule mining strategy and the landscape dynamic change simulation strategy, which has led to insufficient progress in the research concerning these two aspects in recent years.

Two possible ways to combine CA with other artificial intelligence algorithms to obtain better simulation accuracy include: (1) Combination with the agent-based model. The goal of intelligent agent model research is human activities. It is an autonomous model that connects social behavior and land use by simulating individual behavior and pushing up the scale [23]. CA can simulate the spatiotemporal evolution of complex systems, and it is easy to understand and program the model [23]. In recent years, researchers have widely used this model to study land use change and urban expansion [24–26]. The transformation rule is the dynamic basis of the CA simulation of complex system evolution, which influences the simulation process and its results [27,28]. The combination of an agent-based model and CA can significantly improve the predictive ability of the comprehensive model [29]. (2) Combination with the system dynamics model. System dynamics is a discipline that is based on system cybernetics, system theory, and information theory. The feedback structure, function, and dynamic characteristics of the model can be combined with the cellular automata model to analyze the complex system structure of the city from a macro-perspective, resulting in land changes and trends in different scenarios being obtained. System dynamics, combined with CA, for land use change simulation, mainly includes neural network [30–33], rough set algorithm [34], Markov chain [35], genetic algorithm [36,37], ant colony algorithm [38], support vector machine [39], and so on. Both ways have been proven to better support planning policies to achieve sustainable development, but further adjustments are always expected.

This study proposes a patch-generating land use simulation (PLUS) model to combine the Land use Expansion Analysis Strategy (LEAS) and CA model, based on the multi-class random patch seed (CARS) model. This combination contained a new multi-type seed growth mechanism and multi-objective optimization algorithms [40]. As a result, it was expected to gain a better excavation of the inducements of various land use changes.

2. Study Area and Data Sources

2.1. Overview of the Study Area

The study area selected in this paper was the metropolitan area, with Hangzhou as the center, and Shaoxing, Huzhou, Jiaying, Jinhua, Xuancheng, Huangshan, and Quzhou as the sub-centers (See Figure 1). The metropolitan area of Hangzhou is located in the Yangtze

River Delta, one of the most economically active regions in China, accounting for about a quarter of China's total economic output. Dramatic land changes occur there, in order to support its fast economic development. Therefore, the simulation of land use change is urgently needed to provide a theoretical basis for the future planning of the study area and the formulation of relevant policies.

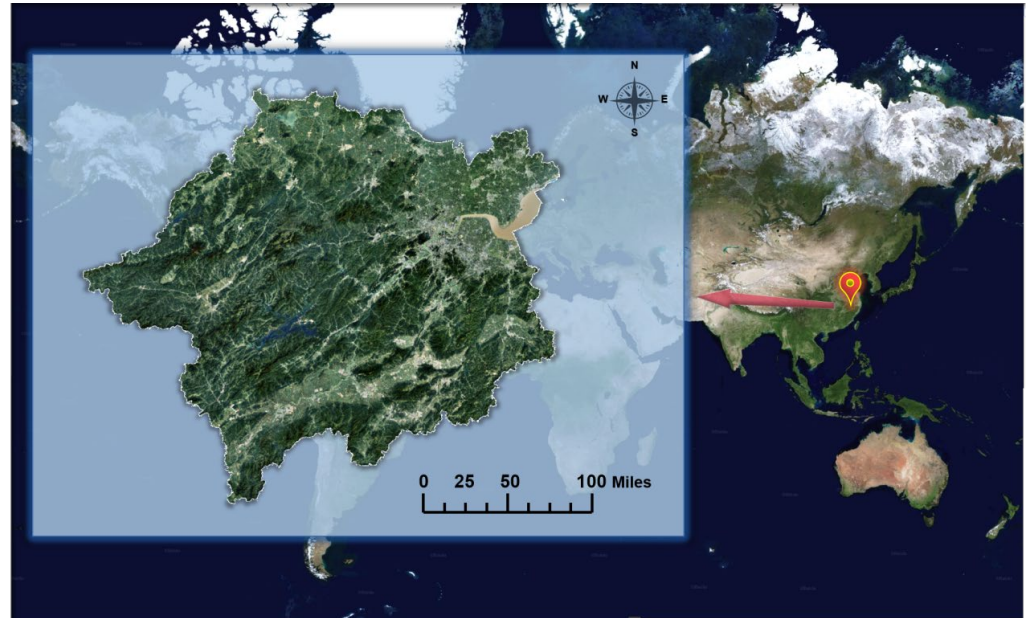


Figure 1. Study area.

The latitude and longitude span of the study area is $28^{\circ}15' \sim 30^{\circ}22' \text{ N}$, $117^{\circ}02' \text{ E} \sim 121^{\circ}16'$. Located in the subtropical monsoon area, it contains a subtropical monsoon climate, with four distinct seasons and abundant rainfall [40]. At present, the total area of the study area is 76,521 square kilometers, including Jiande City, Chun'an County, Tonglu County, Haining City, Tongxiang City, Anji County, Deqing County, She County, Zhuji City, and other county-level cities.

This paper selected the MCD12Q1 data of the study area from 2001 to 2019 as the basic urban land use data. It used these data to perform artificial-intelligence-based urban land use interpretation. For this purpose, the characteristics of the development of other first-tier cities in China and the acquisition of remote-sensing data, were comparatively analyzed. At the same time, the LULC data of the study area in 2005, 2010, 2015, and 2018 were selected as the basic urban land use data. The urban expansion simulation was based on cellular automata.

2.2. Data and Criteria

The data collected and used in this study included data graphs of driving factors such as GDP, subway, digital elevation model (EDM), elevation, highway, river, slope, population, soil, school, and hospital, from 2005, 2010, 2015, and 2018. Moreover, four LULC maps and LULC maps with a resolution of $500 \text{ m} \times 500 \text{ m}$ from 2001 to 2019 were used. The driving-factor data maps were from the Institute of Remote Sensing and Digital Earth, the Chinese Academy of Sciences, and the LULC maps were from USGS. Specifics are shown in Table 1.

Table 1. Summary of data sets.

Data	Criteria	Year	Description	Source	Data Format
Driving factor	GDP	2005 2010 2015 2018	30 arc-rec spatial resolution	Institute of Remote Sensing and Digital Earth, Chinese Academy of Sciences (http://www.radi.cas.cn/index_65411.html (accessed on 10 October 2021))	GeoTIFF
	Subway				
	EDM				
	Elevation				
	Highway				
	River				
	Slope				
	Population				
LULC map	LULC	2001~2019	500 arc-rec spatial resolution	United States Geological Survey (USGS) (https://earthexplorer.usgs.gov/ (accessed on 10 November 2021))	GeoTIFF
		2005 2010 2015 2018	30 arc-rec spatial resolution	United States Geological Survey (USGS) (https://earthexplorer.usgs.gov/ (accessed on 10 November 2021))	GeoTIFF
Administrative map	Hangzhou Shaoxing Huzhou Jiaxing Jinhua Xuancheng Huangshan Quzhou	2021	A satellite image from Landsat, USGS and LAPAN	Ministry of Environment and Forestry, Indonesia (http://webgis.dephut.go.id:8080/kemenhut/index.php/id/fitur/unduh (accessed on 10 November 2021) , https://earthexplorer.usgs.gov/ (accessed on 10 November 2021))	KML

3. Methodology

3.1. LULC Data Processing

The obtained LULC map was spliced in ENVI, then the spliced data were rendered using ArcMap10.7 (the main application used in ArcGIS). Finally, the data type was converted into the corresponding type that the model was able to handle through the PLUS model to complete the preprocessing of the data.

3.2. Introduction of the Patch-Generating Land Use Simulation (PLUS) Model

Step 1: Land use Expansion Analysis Strategy (LEAS) [40] (see Figure 2). This strategy extracts the expansion of various types of land between the two phases of land use change. Moreover, sampling from the added part uses a random forest algorithm to mine the factors of various types of land use expansion and driving forces. As a result, the development probabilities of various types of land and the contribution of driving factors to the expansion of various types of land during this period are obtained. This strategy integrates advantages of the existing TAS and PAS, avoids the analysis of conversion types that increase exponentially with the number of categories, retains the model's ability to analyze the mechanism of land use change within a certain period, and has better interpretability.

Step 2: The CA model is based on multi-class random patch seed (CARS) [40] (see Figure 3). Combining the random seed generation and threshold-decreasing mechanism, the PLUS model can dynamically simulate the automatic generation of plaques in time and space, under the constraints of development probability.

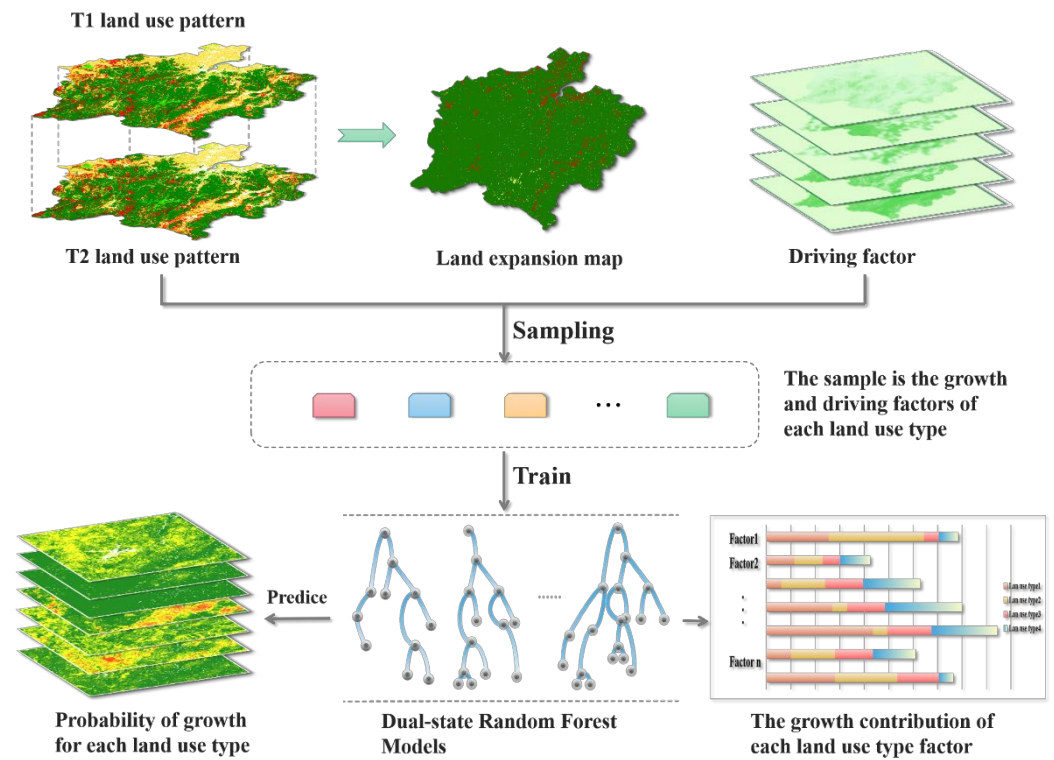


Figure 2. Land use Expansion Analysis Strategy (LEAS).

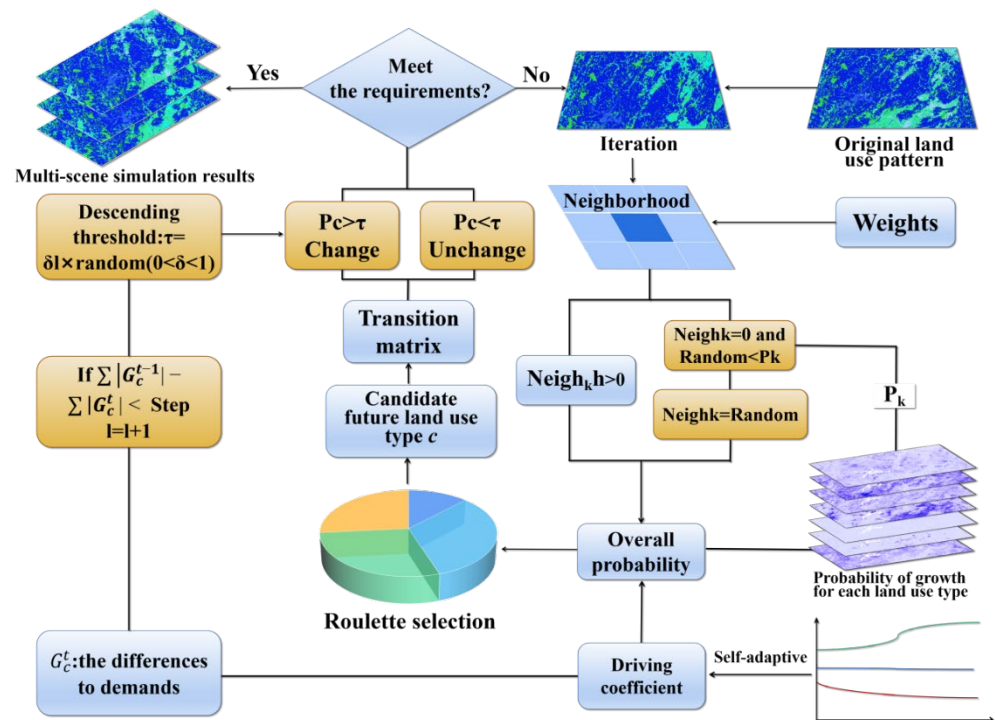


Figure 3. CA model based on multi-class random patch seed (CARS).

The basic formula for the total probability of each land use type is as follows [40]:

$$OP_{i,k}^{d=1,t} = P_{i,k}^{d=1} \times \Omega_{i,k}^t \times D_k^t \quad (1)$$

where $P_{i,k}^{d=1}$ represents the growth probability of type k land use at i ; D_k^t represents the impact of future land use demand of type k , which depends on the gap between the current

amount of land at t and the land use target demand k ; and $\Omega_{i,k}^t$ represents the domain effect of unit i , which is the following neighbor of the coverage ratio of the land use component of k within the domain [40].

$$\Omega_{i,k}^t = \frac{\text{con}(C_i^{t-1} = k)}{n \times n - 1} \times w_k \tag{2}$$

Among them, $\text{con}(C_i^{t-1} = k)$ represents the last iteration. In the window of $n \times n$, w_k represents different land use types having different neighborhood effects. The default value of w_k is 1, but it can be freely defined. The adaptation method is as follows [41]:

$$D_k^t = \begin{cases} D_k^{t-1} \text{ if } |G_k^{t-1}| \leq |G_k^{t-2}| \\ D_k^{t-1} \times \frac{G_k^{t-2}}{G_k^{t-1}} \text{ if } 0 > G_k^{t-2} > G_k^{t-1} \\ D_k^{t-1} \times \frac{G_k^{t-1}}{G_k^{t-2}} \text{ if } G_k^{t-1} > G_k^{t-2} > 0 \end{cases} \tag{3}$$

where the sum is the difference between the number of land use types k , in iterations G_k^{t-1} and G_k^{t-2} and the future demand. Finally, according to the overall probability of all land use types, a wheel is constructed to select the land use status in the next iteration [42].

At the same time, in order to simulate the patch evolution of multiple land use types, a multi-type random patch-seeding mechanism based on threshold drop is adopted, which is realized through a calculation process.

$$OP_{i,k}^{d=1,t} = \begin{cases} P_{i,k}^{d=1} \times (r \times \mu_k) \times D_k^t \text{ if } \Omega_{i,k}^t = 0 \text{ and } r < P_{i,k}^{d=1} \\ P_{i,k}^{d=1} \times \Omega_{i,k}^t \times D_k^t \text{ all others} \end{cases} \tag{4}$$

Among them, r is a random value from 0 to 1, and μ_k is the threshold for generating a new land use patch for k -type land use, which the model user determines in order to control the organic growth and spontaneous growth of multiple land use types. If a new land use type wins a round of competition, a lowered threshold τ is used to evaluate the selected candidate land use types, as follows:

$$\begin{aligned} &\text{If } \sum_{k=1}^N |G_c^{t-1}| - \sum_{k=1}^N |G_c^t| < \text{Step Then, } l = l + 1 \\ &\begin{cases} \text{Change } P_{i,c}^{d=1} > \tau \text{ and } TM_{k,c} = 1 \\ \text{No change } P_{i,c}^{d=1} \leq \tau \text{ or } TM_{k,c} = 0 \end{cases} \end{aligned} \tag{5}$$

Among them, the step length is the step length of the PLUS model, to approximate the land use demand; δ is the attenuation factor of the decreasing threshold τ , ranging from 0 to 1, which the expert sets; $r1$ is the random value of the normal distribution, the mean value is 1, the range is 0~2; l is the number of attenuation steps. $TM_{k,c}$ is the transition matrix, which defines whether the land use type K -type is allowed to be converted to C -type. Through this descending threshold, new land use patches will spontaneously grow and develop freely under the constraints of growth probability [43].

3.3. Selection of Driving Factors

3.3.1. Geomorphology and Geology

The terrain of Zhejiang is high in the southwest and slopes from the southwest to the northeast. The northeast is a low and flat alluvial plain, hills and coastal plains dominate the east, the middle is dominated by hills and basins, and the southwest is dominated by mountains and hills. It can be roughly divided into six terrain areas: the North Zhejiang Plain, the hills and basins in the southwest of Zhejiang, the coastal plains, and the coastal islands in the southeast of Zhejiang. Alluvial plains with dense water networks in northern

Zhejiang, coastal plains and hills in eastern Zhejiang, basins in central Zhejiang, hills and mountains in southwestern Zhejiang, and island landforms in Zhoushan all include various types of landforms. Mountains with sizes over a kilometer mostly surround the southwest. Huangmaojian, located in Longquan, has an elevation of 1929 m, and it is the highest peak in Zhejiang Province. Again, plains, hills, and basins dominate the terrain.

By combining the results of land use classification in the study area, the main built-up areas of the study area are concentrated in the eastern region dominated by plains. In contrast, the cultivated land is concentrated in the southern and northern regions and dominated by low mountains and hills, and woodlands are widely distributed throughout the entire research area. For this reason, the expansion of land use in the study area is mainly concentrated within the eastern, southern, and northern plains and the middle–low mountain areas.

3.3.2. Climatic Settings

Due to the subtropical monsoon climate, the climate characteristics of the study area are high in temperature: the annual average temperature is 15~23 °C. Taking July as the highest temperature, there is much precipitation, with the annual average precipitation being 1200~2000 mm. The rainfall distribution during the year is relatively even, with there being no drought and less rain areas. There is much sunshine, with the annual average sunshine period being more than 1800 h. Sunshine is most abundant from June to December. The wind speed is low: the average wind speed in urban areas is not high, with an average speed of only 1.9 m/s. Except for the wind direction, which directly affects the layout of the industrial land and residential land, other climatic conditions indirectly influence land use distribution in the study area.

3.3.3. Economic Development

Urban expansion and economic development present a cyclical relationship, and most of the expansion of construction land is influenced by economic development. In the Hangzhou metropolitan area, four rounds of urban expansion have been observed. From 1984 to 1985, the first round of rapid economic development since the economic reform caused the first instance of out-of-control land use in most parts of Hangzhou and the surrounding cities. In the subsequent years from 1988 to 1989, from 1993 to 1994, and after 2000, there were three rounds of urban land expansion under the influence of excessive economic growth.

3.3.4. Industrialization Policies

In China, with mixed-use urban planning, the issue of land transfer permits, and government investment in infrastructures and public amenities occurring, governments in Chinese cities have proven their robust control in defining the development of a city [44]. In Hangzhou and the surrounding cities, the local governments have introduced measures for the macro-control of urban expansion, from limiting the supply of construction land, to land planning and design. Although most measures have failed to address the increasing need for construction land during rapid economic development, these policies and measures have defined the direction of legal urban expansion, and they are decisive for certain issues, such as “return farmland to forest”.

4. Results

4.1. Land Use Interpretation

Based on GIS and LULC raster data, processing and analysis were performed to describe land-cover types. Generally speaking, the data set contained 17 main land-cover types. According to the International Geosphere-Biosphere Program (IGBP), this included 11 natural vegetation and 3 land development land types, mosaic land types, and 3 non-vegetable land types. According to the analysis of the study area, it was found that the land-cover types in the study area were mainly limited to 12 to 14 types, as shown in

Figure 4. The specific area changes of each type are shown in Figure 5. The results showed a tremendous increase in urban built-up land from 2001 to 2019, which corresponded to a decrease in the area of farmland and other land types. At the same time, the forest land also increased significantly.

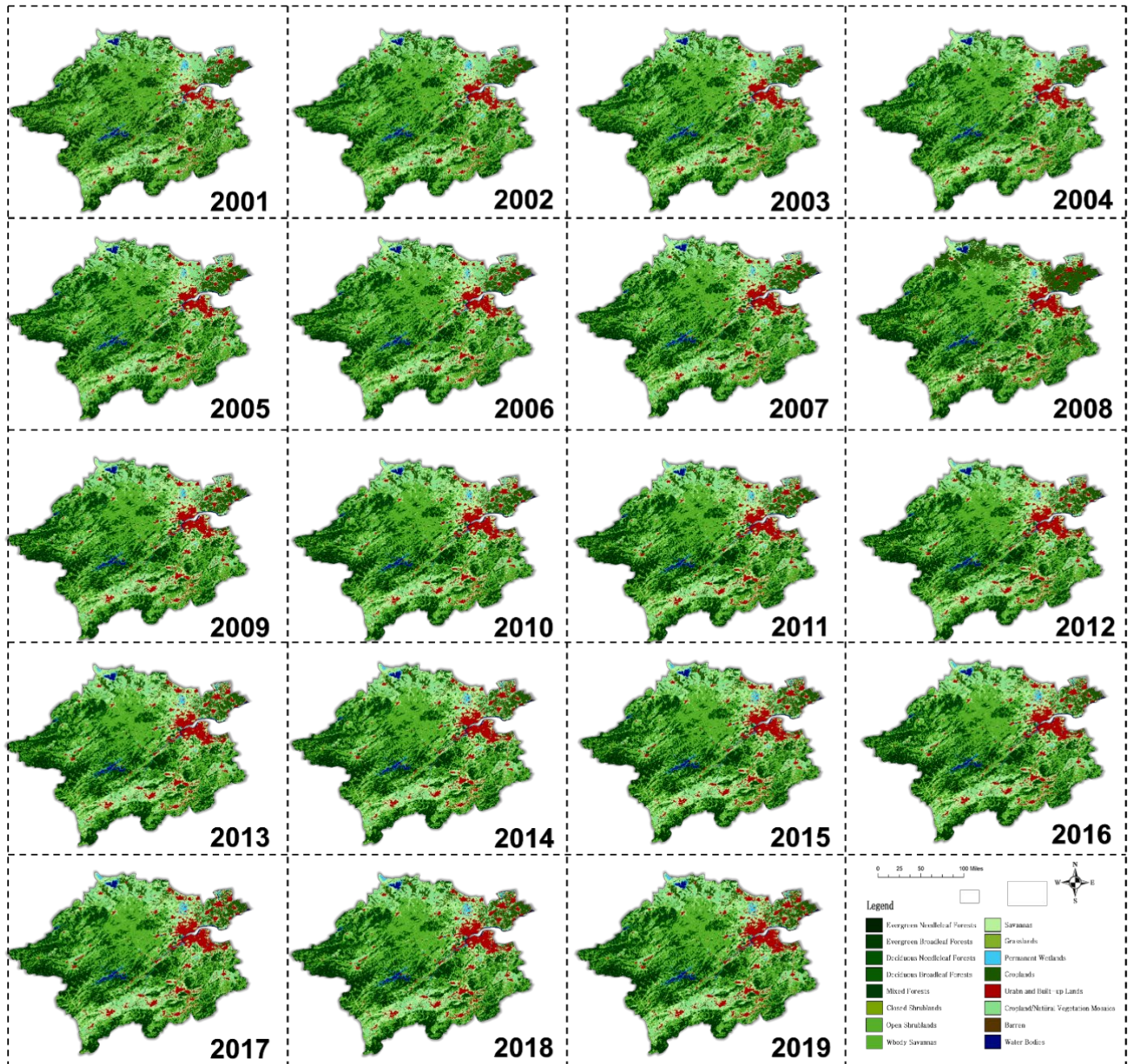


Figure 4. The main land-cover types in the study area from 2001 to 2019.

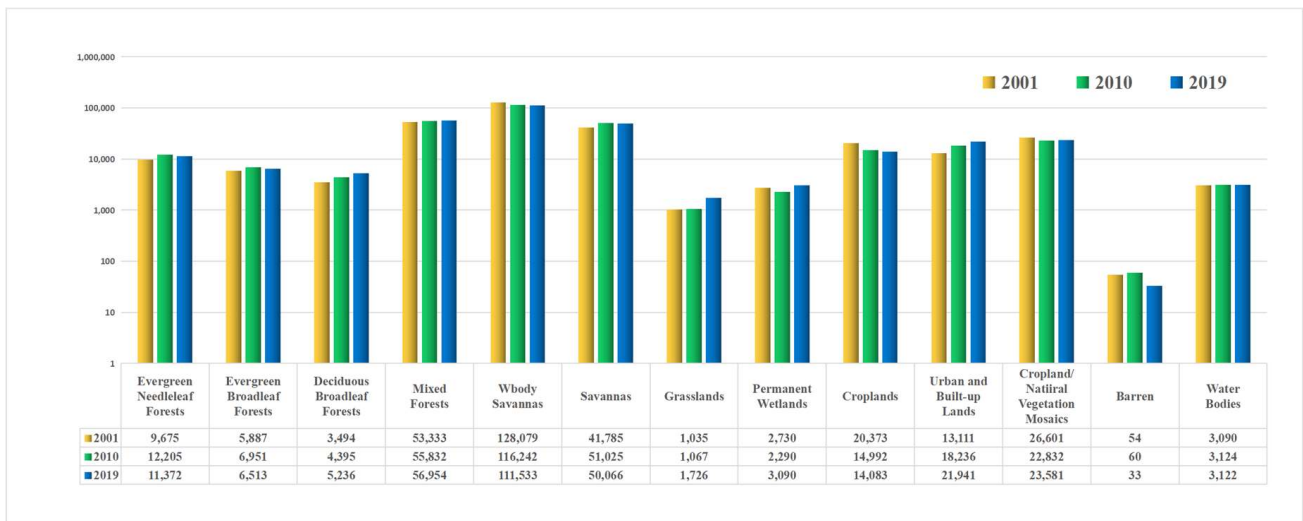


Figure 5. Areas of various types of land use in 2001, 2010, and 2019 (note: some land use types with a very small area are ignored).

4.2. Urban Expansion Simulation Based on PLUS Model

By inputting the LULC map in 2005 and 2010, 2010 and 2015, and 2015 and 2018, and by extracting the expansion of various types of land between the two phases of land use changes in different years in the study area, this study extracted the land use expansion for Zhejiang for different periods, as shown in Figure 6.

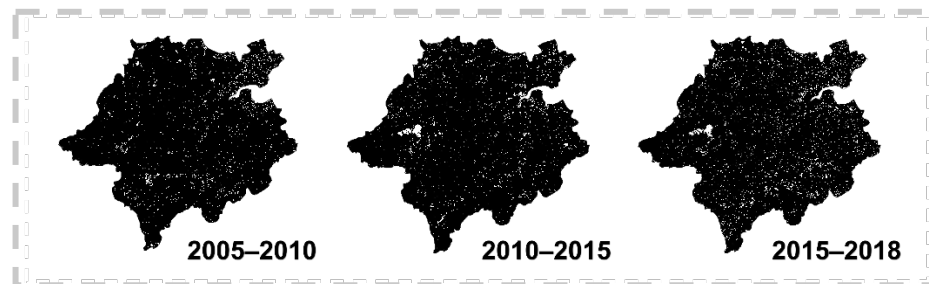


Figure 6. Land use expansion extraction, 2005–2010, 2010–2015, and 2015–2018.

We sampled the additional part obtained from Step 1 and used the random forest algorithm. The sampling methods were uniform sampling and random sampling, and the sampling rate was set to 0.01 to excavate various land uses and driving forces one by one. Eight driving factors were selected for this excavation, including GDP, subway, EDM, elevation, highway, river, slope, population, soil, school, and hospital.

The contribution of all these driving factors to the expansion of various land use types is outputted, as shown in Figures 7–10. The higher the brightness, the greater the contribution rate. As shown, the driving factors had the highest contribution rates toward grassland, forest, farmland, and urban land, and the contribution rates to forest and urban land kept rising.

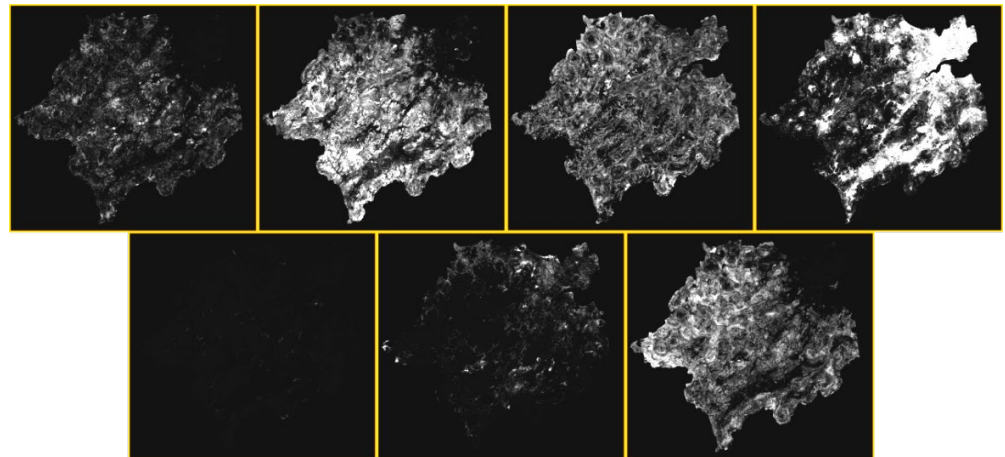


Figure 7. Development probabilities for various types of land, and the contribution of land expansion in 2005–2010 (the clearer the white, the greater the contribution).

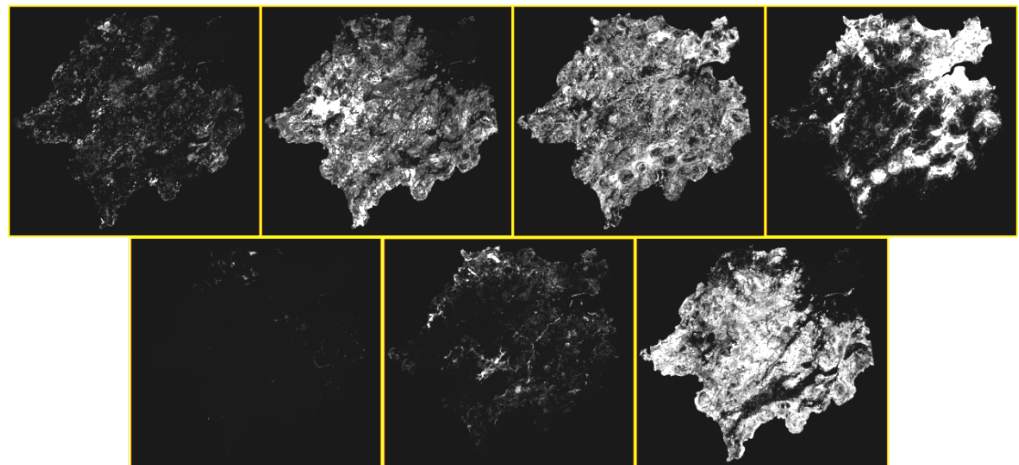


Figure 8. The development probabilities of various types of land, and the contribution of land expansion in 2010–2015 (the clearer the white, the greater the contribution).

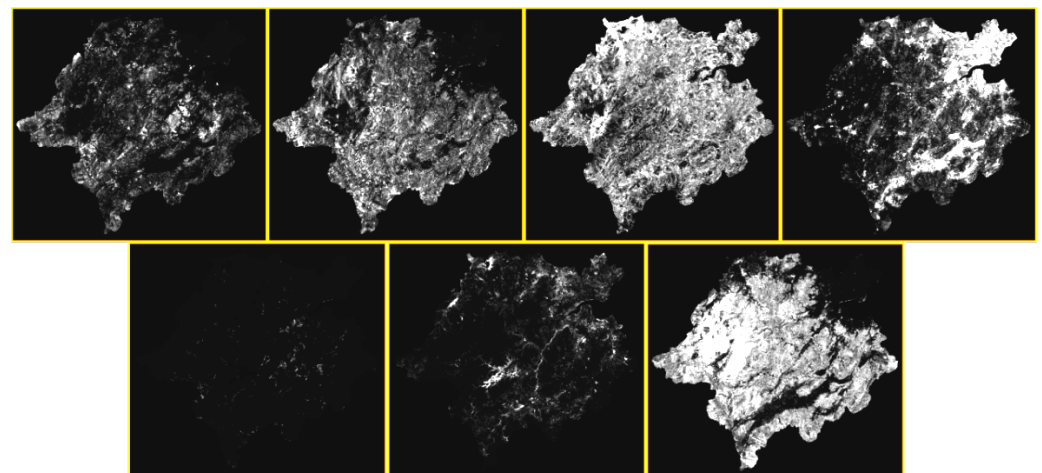


Figure 9. The development probabilities of various types of land, and the contribution of land expansion in 2015–2018 (the clearer the white, the greater the contribution).

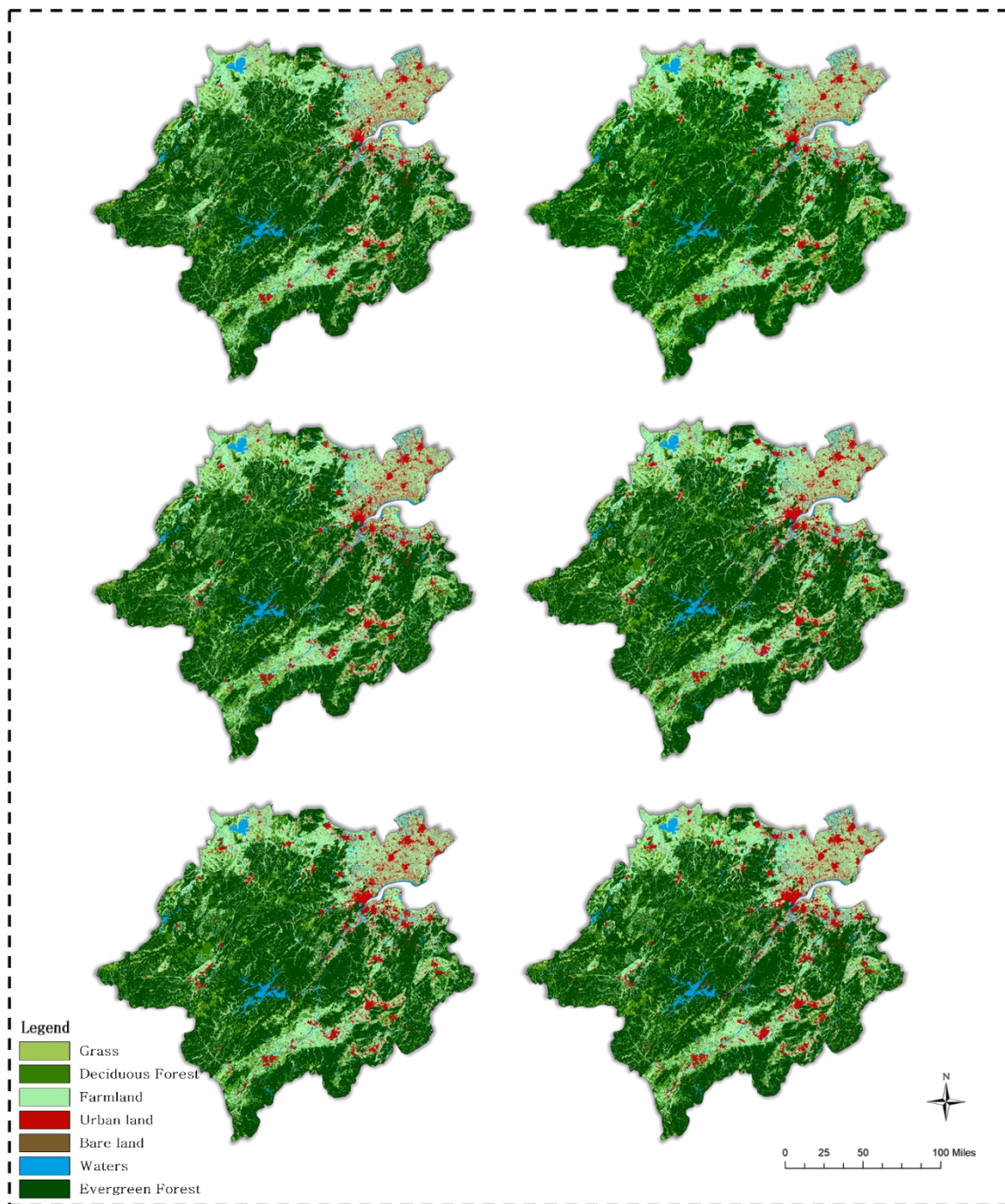


Figure 10. Land expansion simulation and real land use in 2005–2010, 2010–2015, and 2015–2018: A comparison of types.

4.3. Verification of PLUS Model

Combining random seed generation and the threshold-decreasing mechanism, the PLUS model in this study dynamically simulated the automatic generation of plaques in time and space, under the constraints of development probability. The simulation was implemented for 2005–2010, 2010–2015, and 2015–2018 in turn, and the results are shown in Figure 10.

According to the above results, the simulation accuracy was verified, and the results are shown in Table 2. According to the advanced comparison between the PLUS model simulation results and the real land use type data, the results are shown in Table 3.

Table 2. Simulation accuracy verification for 2005–2010, 2010–2015, and 2015–2018.

Year	Kappa Coefficient (%)	User's Accuracy (%)						
		Grass	Deciduous Forest	Cultivated Field	Urban Land	Bare Land	Waters	Evergreen Forest
2005–2010	0.956	0.988	0.976	0.965	0.842	0.954	0.988	0.988
2010–2015	0.918	0.933	0.934	0.929	0.854	0.910	0.925	0.971
2015–2018	0.923	0.944	0.901	0.936	0.891	0.792	0.930	0.976

Table 3. Comparison of the area of the land use type simulation and the real land use type in 2010, 2015, and 2018 (km²).

Year	Grass	Deciduous Forest	Cultivated Field	Urban Land	Bare Land	Waters	Evergreen Forest
2005–2010	2,620,709	8,157,319	23,216,915	4,817,324	15,459	2,151,630	44,151,632
Real (2010)	2,809,602	8,248,160	23,216,938	4,817,326	20,945	2,349,566	43,688,758
2010–2015	2,784,092	8,278,020	22,533,997	5,478,163	10,133	2,338,896	43,727,994
Real (2015)	2,784,850	8,545,279	22,536,173	5,609,103	22,292	2,340,847	43,312,322
2015–2018	2,668,851	8,566,745	22,075,873	5,916,046	19,137	2,327,583	43,576,631
Real (2018)	2,820,751	8,127,297	22,080,545	6,189,235	19,141	2,328,292	43,580,324

According to the above data, the results of the three simulations reached over 80%, the accuracy of centralized urban land use reached over 84%, and the kappa coefficient reached over 91%. Therefore, the accuracy of the model was high.

4.4. Application of PLUS Model for Prediction

According to the data, the study area has, in recent years, reduced mainly in farmland and increased in forest area, as a result of the protection and development of the ecological environment. At the same time, the area of urban land in the study area has been increasing year by year, and the level of urbanization has increased significantly. Therefore, some environmental issues are echoed in the strengthening of ecological civilization within the study area. Based on the above results from the simulation of land use types in 2024, 2027, and 2030, these results are shown in Figure 11, and the specific values are shown in Table 4. According to the simulation of the future years, 2024, 2027, and 2030, it can be seen that the area of urban land in the study area will continue to increase significantly, which may be related to the rapid economic development of the study area in the future. The increase in land use in these cities was mainly achieved by reducing the grassland area, while the changes in area for other types of land use were relatively small.

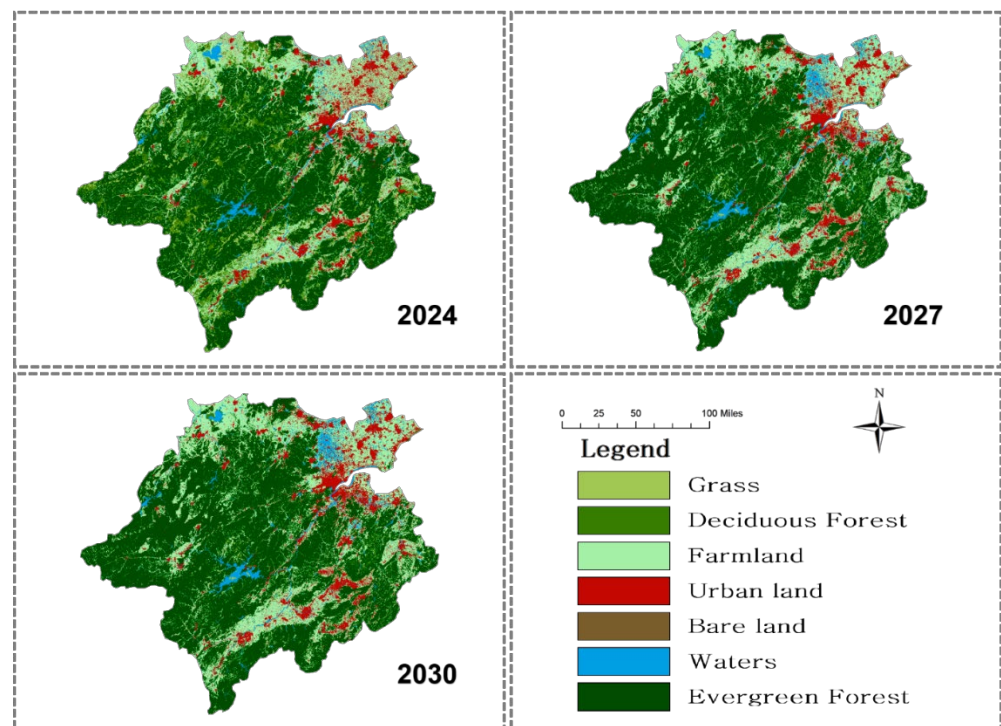


Figure 11. Simulation of land use types in 2024, 2027, and 2030.

Table 4. Simulation of land use types in 2024, 2027, and 2030 (km²).

Year	Grass	Deciduous Forest	Cultivated Field	Urban Land	Bare Land	Waters	Evergreen Forest
2024	2,888,345	7,412,612	21,330,385	7,156,186	14,780	2,305,684	44,025,773
2027	2,919,596	7,107,580	21,029,018	7,560,284	13,299	2,295,743	44,208,246
2030	2,949,129	6,832,732	20,767,392	7,919,104	12,149	2,286,461	44,366,799

5. Conclusions and Discussion

Scholars have long pursued models for better accuracy in predicting land use change. For example, Salem et al. used the logistic regression model to analyze Delhi over the past 30 years, based on various driving factors, but the maximum regression coefficient only reached 0.8646 [45]. Gantumur et al. used CA and an artificial neural network (ANN) to study the urban growth rate of Ulan Bator, but the kappa coefficient only reached barely higher than 70% [46]. The kappa coefficient was raised to 80% and 78% when Pijanowski et al. established a UEM model with GIS, ANN, and RS. ROC curve and kappa statistics were used to conduct a calibration for the study of land use changes in the Tehran metropolitan area [47]. Since then, it seems extremely difficult to increase the accuracy.

This paper interprets and predicts the expansion of seven land use types in the study area from 2001 to 2019, based on the PLUS model, which combines LEAS and CARS. By choosing a variety of driving factors, the PLUS model simulates urban expansion in the metropolitan area of Hangzhou. The results show that the accuracy of the simulation, manifested as the kappa coefficient of urban land, has increased to more than 84%, and the kappa coefficient of other land use types is more than 90%. Compared with other models, such as the cellular automata and Markov chain, this model has better accuracy and can better simulate the future land use changes of the city. Cellular automata and Markov chain are used to study the driving mechanisms of land use change. The results show that economy and policy lead to urban change, compared with population and natural factors. This study further simulates and predicts land use over the next eight years and finds that

except for the fast growth (more than 10.6%) of urban land, grassland and evergreen forest would also grow, at the cost of reducing other types of land use.

To a certain extent, the PLUS model used in this paper solves the CA model's deficiencies in the conversion rule-mining strategy and landscape dynamic change simulation strategy. A new analysis strategy is applied to better uncover the inducements of various land use changes by containing a new multi-type seed growth mechanism that can better simulate multi-type land use patch-level changes. At the same time, coupled with multi-objective optimization algorithms, the simulation results can better support planning policies to achieve sustainable development.

However, this study lacks consideration towards many restrictive factors when considering driving factors, such as topography, which would affect the final accuracy to a certain extent. In the future, there should be more consideration toward restrictive factors. Furthermore, during the research process, it was found that the PLUS model could not effectively simulate long-term land use change. Therefore, a new method for the prediction of long-term land use is still needed, and neural networks or deep-learning methods might be helpful in this regard.

Author Contributions: Conceptualization, L.X., X.L. and L.Y.; methodology, W.Z. and Z.L.; software, L.X. and W.Z.; validation, L.X., D.T. and L.Y.; formal analysis, L.X. and D.T.; data curation, W.Z. and L.Y.; writing—original draft preparation, L.X. and X.L.; writing—review and editing, D.T. and Z.L.; visualization, L.Y.; supervision, D.T.; project administration, D.T. and Z.L.; funding acquisition, D.T. All authors have read and agreed to the published version of the manuscript.

Funding: This research was funded by the Tiehan Project Fund of Laboratory for Urban Future, Peking University (Shenzhen), and jointly supported by the National College Students Innovation and Entrepreneurship Training Program of China (No.202110349021).

Data Availability Statement: The data used in this paper are published open-source data available at http://www.radi.cas.cn/index_65411.html (accessed on 10 October 2021), <https://earthexplorer.usgs.gov/> (accessed on 10 November 2021) and <http://webgis.dephut.go.id:8080/kemenhut/index.php/id/fitur/unduh> (accessed on 10 November 2021).

Conflicts of Interest: The authors declare no conflict of interest.

References

1. UN Department of Economic and Social Affairs. *World Urbanization Prospects: The 2018 Revision*; United Nations: New York, NY, USA, 2018.
2. Haaland, C.; van Den Bosch, C.K. Challenges and strategies for urban green-space planning in cities undergoing densification: A review. *Urban For. Urban Green.* **2015**, *14*, 760–771. [[CrossRef](#)]
3. Rimal, B.; Zhang, L.; Keshtkar, H.; Wang, N.; Lin, Y. Monitoring and modeling of spatiotemporal urban expansion and land use/land-cover change using integrated Markov chain cellular automata model. *ISPRS Int. J. Geo-Inf.* **2017**, *6*, 288. [[CrossRef](#)]
4. Saputra, M.H.; Lee, H.S. Prediction of land use and land cover changes for north sumatra, indonesia, using an artificial-neural-network-based cellular automaton. *Sustainability* **2019**, *11*, 3024. [[CrossRef](#)]
5. Turner, B.; Moss, R.H.; Skole, D.L. Relating land use and global land-cover change. *Glob. Change Rep.* **1993**, *5*, 95.
6. Cegielska, K.; Noszczyk, T.; Kukulska, A.; Szylar, M.; Hernik, J.; Dixon-Gough, R.; Jombach, S.; Valánszki, I.; Kovács, K.F. Land use and land cover changes in post-socialist countries: Some observations from Hungary and Poland. *Land Use Policy* **2018**, *78*, 1–18. [[CrossRef](#)]
7. Kogo, B.K.; Kumar, L.; Koech, R. Analysis of spatio-temporal dynamics of land use and cover changes in Western Kenya. *Geocarto Int.* **2021**, *36*, 376–391. [[CrossRef](#)]
8. Wu, R.; Li, Z.; Wang, S. The varying driving forces of urban land expansion in China: Insights from a spatial-temporal analysis. *Sci. Total Environ.* **2020**, *766*, 142591. [[CrossRef](#)]
9. Zheng, W.; Li, X.; Yin, L.; Wang, Y. Spatiotemporal heterogeneity of urban air pollution in China based on spatial analysis. *Rend. Lincei* **2016**, *27*, 351–356. [[CrossRef](#)]
10. Chen, X.; Yin, L.; Fan, Y.; Song, L.; Ji, T.; Liu, Y.; Tian, J.; Zheng, W. Temporal evolution characteristics of PM_{2.5} concentration based on continuous wavelet transform. *Sci. Total Environ.* **2020**, *699*, 134244. [[CrossRef](#)]
11. Li, X.; Zheng, W.; Yin, L.; Yin, Z.; Xia, T. Influence of social-economic activities on air pollutants in Beijing, China. *Open Geosci.* **2017**, *9*, 314–321. [[CrossRef](#)]
12. Gohain, K.J.; Mohammad, P.; Goswami, A. Assessing the impact of land use land cover changes on land surface temperature over Pune city, India. *Quat. Int.* **2021**, *575*, 259–269. [[CrossRef](#)]

13. Zheng, W.; Li, X.; Yin, L.; Wang, Y. The retrieved urban LST in Beijing based on TM, HJ-1B and MODIS. *Arab. J. Sci. Eng.* **2016**, *41*, 2325–2332. [[CrossRef](#)]
14. Li, X.; Zheng, W.; Lam, N.; Da, N.W.; Yin, Z. Impact of land use on urban water-logging disaster: A case study of Beijing and New York cities. *Environ. Eng. Manag. J.* **2017**, *16*, 1211–1216.
15. Lambin, E.F.; Turner, B.L.; Geist, H.J.; Agbola, S.B.; Angelsen, A.; Bruce, J.W.; Coomes, O.T.; Dirzo, R.; Fischer, G.; Folke, C.; et al. The causes of land use and land-cover change: Moving beyond the myths. *Glob. Environ. Chang.* **2001**, *11*, 261–269. [[CrossRef](#)]
16. Li, X.; Yeh, A.G.O. Neural-network-based cellular automata for simulating multiple land use changes using GIS. *Int. J. Geogr. Inf. Sci.* **2002**, *16*, 323–343. [[CrossRef](#)]
17. Chen, G.; Li, X.; Liu, X.; Chen, Y.; Liang, X.; Leng, J.; Xu, X.; Liao, W.; Qiu, Y.; Wu, Q.; et al. Global projections of future urban land expansion under shared socioeconomic pathways. *Nat. Commun.* **2020**, *11*, 537. [[CrossRef](#)]
18. Clarke, K.C.; Gaydos, L.J. Loose-coupling a cellular automaton model and GIS: Long-term urban growth prediction for San Francisco and Washington/Baltimore. *Int. J. Geogr. Inf. Sci.* **1998**, *12*, 699–714. [[CrossRef](#)]
19. Liu, L.; Li, Z.; Fu, X.; Liu, X.; Li, Z.; Zheng, W. Impact of Power on Uneven Development: Evaluating Built-Up Area Changes in Chengdu Based on NPP-VIIRS Images (2015–2019). *Land* **2022**, *11*, 489. [[CrossRef](#)]
20. Cao, M.; Tang, G.; Shen, Q.; Wang, Y. A new discovery of transition rules for cellular automata by using cuckoo search algorithm. *Int. J. Geogr. Inf. Sci.* **2015**, *29*, 806–824. [[CrossRef](#)]
21. Sohl, T.L.; Claggett, P.R. Clarity versus complexity: Land-use modeling as a practical tool for decision-makers. *J. Environ. Manag.* **2013**, *129*, 235–243. [[CrossRef](#)]
22. Yang, J.; Gong, J.; Tang, W.; Liu, C. Patch-based cellular automata model of urban growth simulation: Integrating feedback between quantitative composition and spatial configuration. *Comput. Environ. Urban Syst.* **2020**, *79*, 101402. [[CrossRef](#)]
23. Xu, Q.; Wang, Q.; Liu, J.; Liang, H. Simulation of land-use changes using the partitioned ANN-CA model and considering the influence of land-use change frequency. *ISPRS Int. J. Geo-Inf.* **2021**, *10*, 346. [[CrossRef](#)]
24. Li, X.; Liu, X.P. Case-based cellular automaton for simulating urban development in a large complex region. *Acta Geogr. Sin.* **2007**, *62*, 1097–1109.
25. Wu, D.; Wang, R.; Gao, S.; Ding, W.; Wang, W.; Ge, X.; Liu, J. Simulation and scenario analysis of arable land dynamics in Yellow River Delta. *Trans. Chin. Soc. Agric. Eng.* **2010**, *26*, 285–290.
26. Liu, X.; Liang, X.; Li, X.; Xu, X.; Ou, J.; Chen, Y.; Pei, F. A future land use simulation model (FLUS) for simulating multiple land use scenarios by coupling human and natural effects. *Landsch. Urban Plan.* **2017**, *168*, 94–116. [[CrossRef](#)]
27. Zhou, C.H.; Ou, Y.; Ma, T.; Qin, B. Theoretical perspectives of CA-based geographical system modeling. *Prog. Geogr.* **2009**, *28*, 833–838.
28. White, R.; Engelen, G. Cellular automata and fractal urban form: A cellular modelling approach to the evolution of urban land-use patterns. *Environ. Plan. A* **1993**, *25*, 1175–1199. [[CrossRef](#)]
29. Agyemang, F.S.; Silva, E.; Fox, S. Modelling and simulating ‘informal urbanization’: An integrated agent-based and cellular automata model of urban residential growth in Ghana. *Environ. Plan. B Urban Anal. City Sci.* **2022**. [[CrossRef](#)]
30. Zhou, Y.; Zhang, F.; Du, Z.; Ye, X.; Liu, R. Integrating cellular automata with the deep belief network for simulating urban growth. *Sustainability* **2017**, *9*, 1786. [[CrossRef](#)]
31. Devendran, A.A.; Lakshmanan, G. Analysis and prediction of urban growth using neural-network-coupled agent-based cellular automata model for Chennai Metropolitan Area, Tamil Nadu, India. *J. Indian Soc. Remote Sens.* **2019**, *47*, 1515–1526. [[CrossRef](#)]
32. Wu, X.; Liu, X.; Zhang, D.; Zhang, J.; He, J.; Xu, X. Simulating mixed land use change under multi-label concept by integrating a convolutional neural network and cellular automata: A case study of Huizhou, China. *GISci. Remote Sens.* **2022**, *59*, 609–632. [[CrossRef](#)]
33. Zhang, X.; Zhou, J.; Song, W. Simulating urban sprawl in China based on the artificial neural network-cellular automata-Markov model. *Sustainability* **2020**, *12*, 4341. [[CrossRef](#)]
34. Parvinnezhad, D.; Delavar, M.R.; Pijanowski, B.C.; Claramunt, C. Integration of adaptive neural fuzzy inference system and fuzzy rough set theory with support vector regression to urban growth modelling. *Earth Sci. Inform.* **2021**, *14*, 17–36. [[CrossRef](#)]
35. Gharaibeh, A.; Shaamala, A.; Obeidat, R.; Al-Kofahi, S. Improving land use change modeling by integrating ANN with Cellular Automata-Markov Chain model. *Heliyon* **2020**, *6*, 05092. [[CrossRef](#)]
36. Wang, R.; He, Q.; Zhang, L.; Wang, H. Coupling Cellular Automata and a Genetic Algorithm to Generate a Vibrant Urban Form—A Case Study of Wuhan, China. *Int. J. Environ. Res. Public Health* **2021**, *18*, 11013. [[CrossRef](#)]
37. Momeni, E.; Antipova, A. Pattern-based calibration of cellular automata by genetic algorithm and Shannon relative entropy. *Trans. GIS* **2020**, *24*, 1447–1463. [[CrossRef](#)]
38. Ma, S.; Liu, F.; Ma, C.; Ouyang, X. Integrating logistic regression with ant colony optimization for smart urban growth modelling. *Front. Earth Sci.* **2020**, *14*, 77–89. [[CrossRef](#)]
39. Naghadehi, S.; Asadi, M.; Maleki, M.; Tavakkoli-Sabour, S.M.; Van Genderen, J.L.; Saleh, S.S. Prediction of Urban Area Expansion with Implementation of MLC, SAM and SVMs’ Classifiers Incorporating Artificial Neural Network Using Landsat Data. *ISPRS Int. J. Geo-Inf.* **2021**, *10*, 513. [[CrossRef](#)]
40. Liang, X.; Guan, Q.; Clarke, K.C.; Liu, S.; Wang, B.; Yao, Y. Understanding the drivers of sustainable land expansion using a patch-generating land use simulation (PLUS) model: A case study in Wuhan, China. *Comput. Environ. Urban Syst.* **2021**, *85*, 101569. [[CrossRef](#)]

41. Gu, C.; Hu, L.; Zhang, X.; Wang, X.; Guo, J. Climate change and urbanization in the Yangtze River Delta. *Habitat Int.* **2011**, *35*, 544–552. [[CrossRef](#)]
42. Zhou, L.; Dang, X.; Sun, Q.; Wang, S. Multi-scenario simulation of urban land change in Shanghai by random forest and CA-Markov model. *Sustain. Cities Soc.* **2020**, *55*, 102045. [[CrossRef](#)]
43. Verburg, P.H.; Overmars, K.P. Combining top-down and bottom-up dynamics in land use modeling: Exploring the future of abandoned farmlands in Europe with the Dyna-CLUE model. *Landsc. Ecol.* **2009**, *24*, 1167–1181. [[CrossRef](#)]
44. Tong, D.; Chu, J.; Han, Q.; Liu, X. How Land Finance Drives Urban Expansion under Fiscal Pressure: Evidence from Chinese Cities. *Land* **2022**, *11*, 253. [[CrossRef](#)]
45. Salem, M.; Bose, A.; Bashir, B.; Basak, D.; Roy, S.; Chowdhury, I.R.; Alsalman, A.; Tsurusaki, N. Urban Expansion Simulation Based on Various Driving Factors Using a Logistic Regression Model: Delhi as a Case Study. *Sustainability* **2021**, *13*, 10805. [[CrossRef](#)]
46. Gantumur, B.; Wu, F.; Vandansambu, B.; Tsegmid, B.; Dalaibaatar, E.; Zhao, Y. Spatiotemporal dynamics of urban expansion and its simulation using CA-ANN model in Ulaanbaatar, Mongolia. *Geocarto Int.* **2022**, *37*, 494–509. [[CrossRef](#)]
47. Pijanowski, B.C.; Tayyebi, A.; Delavar, M.R.; Yazdanpanah, M.J. Urban expansion simulation using geospatial information system and artificial neural networks. *Int. J. Environ. Res.* **2009**, *3*, 493–502.